Eur. Phys. J. B **1**, 77–86 (1998)

THE EUROPEAN PHYSICAL JOURNAL B

© EDP Sciences
Springer-Verlag 1998

Structural properties of charged diblock copolymer solutions

P. Guenoun[1,a], M. Delsanti[2], D. Gazeau[2], J.W. Mays[3], D.C. Cook[3], M. Tirrell[4], and L. Auvray[5]

[1] Service de Physique de l'Etat Condensé, C.E.A. Saclay, 91191 Gif-sur-Yvette Cedex, France
[2] Service de Chimie Moléculaire, C.E.A. Saclay, 91191 Gif-sur-Yvette Cedex, France
[3] Department of Chemistry, University of Alabama at Birmingham, Birmingham, Alabama 35294, USA
[4] Department of Chemical Engineering and Materials Science, University of Minnesota, Minneapolis, Minnesota 55455, USA
[5] Laboratoire Léon Brillouin, C.E.A. Saclay, 91191 Gif-sur-Yvette Cedex, France

Received: 19 June 1997 / Received in final form: 4 September 1997 / Accepted: 9 October 1997

Abstract. Aqueous micellar solutions of ionic/neutral block copolymers have been studied by light scattering, small angle neutron scattering and small angle X-ray scattering. We made use of a polymer comprised of a short hydrophobic block (polyethylene-propylene) PEP and of a long polyelectrolytic block (polystyrene-sulfonate) PSSNa which has been shown previously to micellize in water. The apparent polydispersity of these micelles is studied in detail, showing the existence of a few large aggregates coexisting with the population of micelles. Solutions of micelles are found to order above some threshold in polymer concentration. The order is liquid-like, as demonstrated by the evolution with concentration of the peak observed in the structure factor ($q_{\rm peak} \propto c^{1/3}$), and the degree of order is found to be identical over a large range of concentrations (up to 20 wt%). Consistent values of the aggregation number of the micelles are found by independent methods. The effect of salt addition on the order is found to be weak.

PACS. 61.25.Hq Macromolecular and polymer solutions; polymer melts; swelling – 83.70.Hq Heterogeneous liquids: suspensions, dispersions, emulsions, pastes, slurries, foams, block copolymers, etc. – 61.20.Qg Structure of associated liquids: electrolytes, molten salts, etc.

1 Introduction

Diblock copolymers, comprised of a long and nearly fully charged moiety and of a short hydrophobic moiety, may be viewed as polyelectrolytes which are hydrophobically modified. In that respect, they can be considered as very convenient tools for tethering charged chains together and forming new interfacial structures [1]. This may be achieved by adsorbing the water insoluble block onto a surface [2] or, thanks to the self-assembly of such diblocks, in films [3] and in water solution in the form of micelles.

Only a few studies are now available on such systems although first pioneering studies in this field were started about thirty years ago [4]. Selb and Gallot studied systems comprised of cationic polyvinylpyridine salts with polystyrene as the hydrophobic block [5]. Tuzar and his collaborators [6] and Eisenberg's group [7] have studied systems comprised of polystyrene cores with, respectively, poly(methacrylic acid) or sodium polyacrylate coronas, whereas we investigated diblocks of poly(tert-butylstyrene) and poly(styrene sulfonate) [8]. This paper is devoted to the study of such micellar solutions in order to better characterize them by standard techniques such as light, X-ray and neutron scattering. We show how the existence of such micelles is revealed by light scattering and we explain the actual meaning of the measured polydispersity of the system.

The polydispersity of polymeric micellar systems is usually assumed to be low (at least for neutral systems) [9] but recent theories suggest a different situation [10] and direct experimental confirmations are scarce [11]. A few experimental studies (both for neutral and charged systems) already suggest that a more complicated pattern may exist where micelles coexist with both larger aggregates and free chains [12]. We confirm this behavior and defined procedures in order to get reliable measurements of the size and mass of the micelles. We then show that a more accurate view of the interactions between micelles can be obtained by neutron scattering. Such micelles resemble to charged brushes of spherical symmetry [13] thus providing a system mimicking colloids protected by charged grafted chains. Such colloids, which could be stabilized either by grafting of chains or adsorption of diblocks such as the ones under study in this paper, are of wide industrial relevance due to the increased need of water solvated systems. The protection by charged chains is indeed believed to be very efficient against coagulations induced by variations of the ionic strength of the solvent [14]. Interactions between these colloids govern their stability and such interactions can be studied thanks to the micelles. These micelles are shown to order above some concentration in

[a] e-mail: pguenoun@cea.fr

such a way that they exhibit a correlated liquid-like structure whose order is measured. The quality of this order stays surprisingly constant up to high concentrations (at least 20 wt%) in contrast to the behavior of homopolyelectrolytes where correlations exist at a smaller spatial scale and are destroyed at even lower concentrations [15]. Similar examples of liquid order are indeed also found in the area of stabilized colloids [16]. Addition of electrolyte has little influence on the ordering of the micelles, which is a confirmation of the relative insensitivity of such spherical charged brushes to the addition of electrolyte. On the contrary, both polyelectrolytes and colloids are generally disordered upon addition of salt.

2 Experiments

2.1 Materials

Diblock copolymer of poly(ethylene-propylene)-sodium poly(styrene-sulfonate) (PEP/NaPSS) was synthesized as follows. Styrene was polymerized in benzene at room temperature using sec-butyllithium as initiator (standard high vacuum conditions and all-glass reactors were used in this work). After complete conversion of styrene (*ca.* 48 hours), a small amount of isoprene was added to form the desired asymmetric diblock copolymer and polymerization was terminated by addition of methanol. The product was characterized by size exclusion chromatography (SEC) and ^{1}H-NMR for determination of weight average molecular weight (M_W), polydispersity (M_W/M_N) and composition. Values of $M_W = 2.7 \times 10^4$ g/mole, M_W/M_N=1.04, and 87.3 wt% styrene were obtained. The polyisoprene segment was converted to PEP by hydrogenation in xylene using p-toluenesulfonylhydrazide in the presence of Irganox 1010 [17]. SEC and NMR, respectively, confirmed a lack of polymer degradation and complete saturation of the polydiene. The polystyrene block was then sulfonated using an SO_3/triethylphosphate complex [17] and neutralized with sodium methoxide. Elemental analysis for sulfur indicated 89 mol% sulphonation of the PS segments. This diblock is highly asymmetric (about 227 NaPSS units and about 50 PEP units) and has a total M_W of about 4.7×10^4 g/mole:

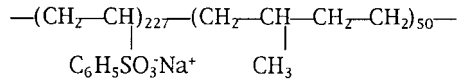

NaPSS homopolymer of $M_W = 4.6 \times 10^4$ g/mole, purchased from Pressure Chemical, was also used. The polydispersity index is smaller than 1.1 and the nominal degree of sulfonation is 1.

Solutions were prepared in deionized H_2O water upon passing it through MilliQ Millipore system of pore size 0.22 μm (18 MΩcm) or in D_2O water. Samples with salt were prepared with NaCl of analytical grade. All the measurements were performed at temperatures close to 25 °C which are above the glass transition temperature of the PEP part ($T_g \approx -60$ °C) [18].

2.2 Quasi-elastic light-scattering

Samples (in H_2O solvent) were filtered through 0.4 or 0.6 μm Nuclepore filters, before being transfered into the scattering cell (8 or 13 mm inner diameter), and centrifuged. Reproducible results were found over several months with the same samples. Light-scattering experiments were carried out at a wavelength $\lambda = 514.5$ nm with a vertically polarized beam. The scattered light was detected with a Brookhaven goniometer BI200SM. A detailed description of the goniometer has been given elsewhere [19]. The correlators used were BI2030AT and BI9000AT correlators.

A large number of correlation functions were accumulated during short periods of time T. The normalized correlation function of the scattered intensity was obtained by summation of the different correlograms with elimination of spurious results due to the presence of dust particles in the scattering volume:

$$\langle I(t)I(0)\rangle/\langle I\rangle^2 = \sum_k \langle I_k(t)I_k(0)\rangle_T / \left(\sum_k \langle I_k\rangle_T\right)^2, \quad (1)$$

where angular brackets $\langle ...\rangle_T$ represent time-averages over time T. The normalized time autocorrelation function of the scattered electric field, $g(t)$, was extracted from the measured time-averaged autocorrelation function of the scattered intensity $\langle I(t)I(0)\rangle$ [19]:

$$g(t) = B[(\langle I(t)I(0)\rangle/\langle I\rangle^2) - 1]^{1/2}. \quad (2)$$

The dimensionless factor B depends on the geometry of the experiment. The experimental quantities $g(t)$ were analyzed by the cumulants method [19] to extract the mean decay rate $\langle\Gamma\rangle_\Gamma$ of $g(t)$ and its variance $v = (\langle\Gamma^2\rangle_\Gamma - \langle\Gamma\rangle_\Gamma^2)/\langle\Gamma\rangle_\Gamma^2$ which measures the deviation from an exponential decay. In order to determine the distribution, $A(\Gamma)$, of the decay rates Γ defined by $g(t) = \int \mathrm{A}(\Gamma) \times \exp(-\Gamma t)\mathrm{d}\Gamma$, a maximum entropy method was used [20]. Experiments were performed at scattering angles between 30° and 135° which corresponds to scattering vectors q ranging from 8.4×10^{-3} nm^{-1} to 3×10^{-2} nm^{-1}.

2.3 Intensity measurements

2.3.1 Light-scattering

The goniometer used and the sample clarification procedure were identical to the ones reported in Section 2.2. The intensities scattered by the copolymer solutions were normalized by the scattering intensity from a benzene sample, $\langle I_B\rangle$, and converted to an apparent weight-average molecular weight as:

$$M_w^{app}(c,q) = \langle I_p(c,q)\rangle/Kc\langle I_B\rangle, \quad (3)$$

where $\langle I_{\rm p}(c,q)\rangle$ is the intensity scattered by the copolymer. In the experiments we conducted, the intensity scattered by the solvent is negligible ($I_{\rm solvent}/\langle I_{\rm p}(c,q)\rangle \leq 3\times 10^{-2}$) and thus $\langle I_{\rm p}(c,q)\rangle$ is identical to $\langle I(c,q)\rangle$, the intensity scattered by the solution, within the experimental error. In this section, c is the concentration expressed in g/cm^3, c(g/cm^3) $= 100c$(wt%), since H_2O is the solvent. The constant K is

$$K = 4\pi^2 n^2 \left(\frac{{\rm d}n}{{\rm d}c}\right)\left(\frac{1}{N_{\rm A}\lambda^4}\right)\left(\frac{1}{R_{\rm B}}\right)\left(\frac{n_{\rm B}}{n}\right)^2, \qquad (4)$$

$R_{\rm B}(=3.0\times 10^5$ cm$^{-1})$ and $n_{\rm B}(=1.5011)$ are the Rayleigh factor and the the index of refraction of benzene, respectively [21]. The refractive index increment of the copolymer (dn/dc) at constant chemical potential at $\lambda =$ 514.5 nm is found to be 0.18 cm^3/g at a salinity of 2×10^{-2} M and in pure water. This value is identical to the value found for PSSNa (0.18 cm^3/g) within the experimental errors. This enables to use with confidence equations (3, 4) since the PEP influence in the dn/dc appears low. Moreover an estimation of the dn/dc of the PEP part alone gives 0.18 cm^3/g, confirming that a single value of index increment can be used.

2.3.2 X-ray scattering

The diffraction patterns were recorded on a small angle X-ray scattering camera with pinhole geometry. The source was a copper rotating anode ($\lambda = 0.154$ nm), with an apparent size of 1 mm $\times$ 1 mm. A detailed description of the camera was given elsewhere [22]. The samples in H_2O were contained in poly(methyl methacrylate) cells of thickness $t_{\rm s} = 1$ mm, closed with Kapton® windows. The measurements were performed with a two-dimensional gas detector located at a distance D (2.1 m) from the sample. The scattering vectors investigated in these experiments range from 10^{-1} to 4 nm^{-1}. As efficiencies of the cells of the detector are equivalent, the scattered intensity $I(q)$ of the sample (cross section per unit scattering volume) can be directly obtained by applying the definition $I(q) = D^2 {\rm I_s}/{\rm I_t} A t_{\rm s}$ where $I_{\rm s}$ and $I_{\rm t}$ represent the intensity scattered by the sample and the transmitted intensity, respectively. The quantity $At_{\rm s}$ is the scattering volume of cross section A times the thickness $t_{\rm s}$. Practically $I(q)$ was obtained as follows:

$$I(q) = D^2(n_{\rm s}/a^2)/n_{\rm t}t_{\rm s} \qquad (5)$$

where $n_{\rm t}$ corresponds to the total number of transmitted photons during the experiment, a^2 is the area of a detector cell (3.24×10^{-6} mm^2) and $n_{\rm s}$ represents the number of photons collected by a detector cell, after subtraction of the photons scattered by Kapton® windows.

2.3.3 Neutron scattering

Neutron scattering experiments were performed on the small angle spectrometer PACE using two sets of wavelength, λ, and sample to detector distance, D, ($\lambda/D = 0.648$ nm/3.0 m and $\lambda/D = 1.4$ nm/4.66 m). Complementary experiments were performed on PAXE spectrometer using the following sets for λ/D : $\lambda/D =$ 0.5 nm/5 m, and $\lambda/D = 1.2$ nm/5 m. Both spectrometers are located at the Laboratoire Léon Brillouin of Saclay, France. With these different configurations, we covered the scattering vector range $3\times 10^{-2} - 1$ nm^{-1}.

The sample cells were quartz cells of inner thickness 2 mm. The scattered intensities were corrected for the parasitic intensity scattered by the quartz cell by subtraction and normalization to the water scattered intensity (in order to eliminate differences in the detector efficiency). The absolute scattering cross section per unit volume $I(q)$ of the sample was determined according to the following formula

$$I(q) = \{[I_{\rm s}/t_{\rm s}T_{\rm s}]/[I_{\rm w}/t_{\rm w}T_{\rm w}]\}{\rm d}\Sigma_{\rm w}/{\rm d}\Omega. \qquad (6)$$

The subscripts s and w correspond to the copolymer sample and to the water sample, respectively, T_i is the transmission of the i-th sample having a thickness t_i, I_i represents the scattered intensity corrected from parasitic scattering and ${\rm d}\Sigma_{\rm w}/{\rm d}\Omega$ is the scattering cross section per unit volume of water deduced from the transmission $T_{\rm w}$ of water [23].

3 Results and discussion

3.1 Dilute solutions

In this section, we present and discuss the results obtained on samples having concentrations smaller than 0.8 wt%. The salinity of the solutions was of the order of 2×10^{-2} M except in the case of neutron measurements where solutions at different salinities were prepared.

Characterization of the solutions by laser light-scattering experiments and especially the q-dependencies of the different measured quantities show the existence of a bimodal population of scatterers. In Figure 1, the intensity scattered by a dilute sample ($c = 2\times 10^{-2}$ wt%) for which interactions are negligible is reported. For $q^2 > 5\times 10^{-4}$ nm^{-2}, the intensity is slightly q^2-dependent whereas at small q values the intensity dramatically increases. The strong curvature observed can only be explained by the presence of a small amount of very large scatterers and a large amount of small scatterers [24]. This point is confirmed by dynamic light-scattering measurements on the same sample. The apparent diffusion coefficient $D^{\rm app}(q) = \langle\Gamma\rangle_\Gamma/q^2$ and the variance v of the decay rate both present a strong q-dependence at small q values (see Fig. 2). These results have been obtained with a linear sample time spacing. The sample time spacing Δt was continuously decreased and the values, reported in Figure 2, correspond to an extrapolation at $\Delta t = 0$ of the apparent quantities measured at different sample time spacings. For $q^2 > 5\times 10^{-4}$ nm^{-2}, these both quantities reach a constant value which indicates that, in this q range, the signal is mainly due to the smaller scatterers. Through the Einstein relation $D^{\rm app}(q > 2.2\times 10^{-2}\ {\rm nm}^{-1}) = k_{\rm B}T/6\pi\eta R_{\rm shz}$,

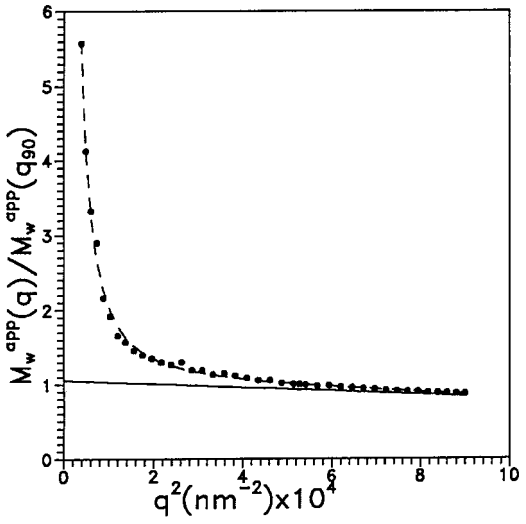

Fig. 1. Apparent weight-average molecular weight *versus* q^2 for a dilute solution where interactions are negligible ($c = 2 \times 10^{-2}$ wt% and salinity 2×10^{-2} M). This behavior clearly shows that two populations of scatterers are present: a small amount of large scatterers and a large amount of small scatterers. The dashed line represents the best fit using expression (8). The solid line represents the contribution of the smaller scatterers.

where $R_{\rm shz}$ is a mean hydrodynamic radius and η the viscosity of the water, one deduces that the size $R_{\rm shz}$ of the smaller scatterers is of the order of 40 nm.

To test quantitatively the hypothesis of the existence of a bimodal population, different treatments of the data were performed. If this hypothesis is correct, the apparent average molecular weight $M_{\rm w}^{\rm app}(q)$ deduced from intensity light-scattering should have the following form,

$$M_{\rm w}^{\rm app}(q) = w_{\rm l} M_{\rm lw} P_{\rm lz}(q) + w_{\rm s} M_{\rm sw} P_{\rm sz}(q), \quad \text{with } w_{\rm s} = 1 - w_{\rm l} \tag{7}$$

where $M_{i\rm w}$ and w_i are the weight-average molecular weight and the weight fraction of the different scatterers. Indices $i =$ s or l correspond to smaller and larger scatterers respectively and $P_{iz}(q)$ represents the z-average form factor of the i-th scatterer. From the numerical value of $R_{\rm shz}$, it is meaningful to assume that the z-average radius of gyration of the smaller scatterers $R_{\rm sgz}$ is such that $qR_{\rm sgz} \leq 1$. Thus the form factor $P_{\rm sz}(q)$ can be approximated by $1 - q^2R_{\rm sgz}^2/3$. The strong upper curvature of $M_{\rm w}^{\rm app}(q)$ indicates a regime where $qR_{\rm lgz}$ is much larger than 1, where $R_{\rm lgz}$ is the z-average radius of gyration of the larger scatterers. Thus we made the reasonable choice to approximate $P_{\rm lz}(q)$ by a power law $P_{\rm lz}(q) \propto 1/q^x$ with $1 \leq x \leq 4$. The various values of x correspond to different possible structures of the larger scatterers. The q-dependence of the dissymetry of the measured scattered intensity $M_{\rm w}^{\rm app}(q)/M_{\rm w}^{\rm app}(q_{90^\circ})$ (Fig. 1) was successfully fitted to the following profile:

$$M_{\rm w}^{\rm app}(q)/M_{\rm w}^{\rm app}(q_{90^\circ}) = B_{\rm l}/q^x + B_{\rm s}(1 - \frac{q^2R_{\rm sgz}^2}{3}). \tag{8}$$

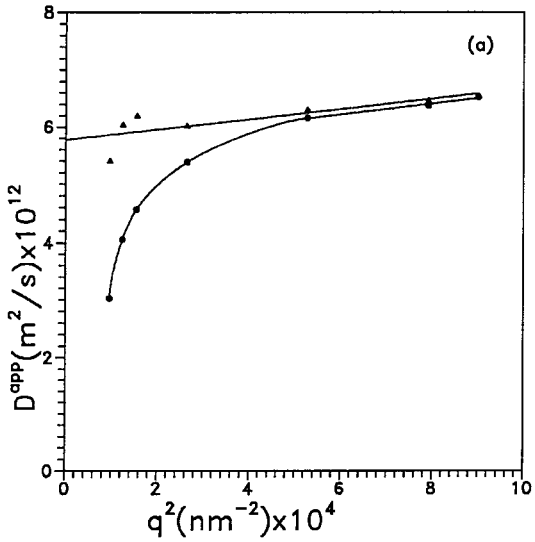

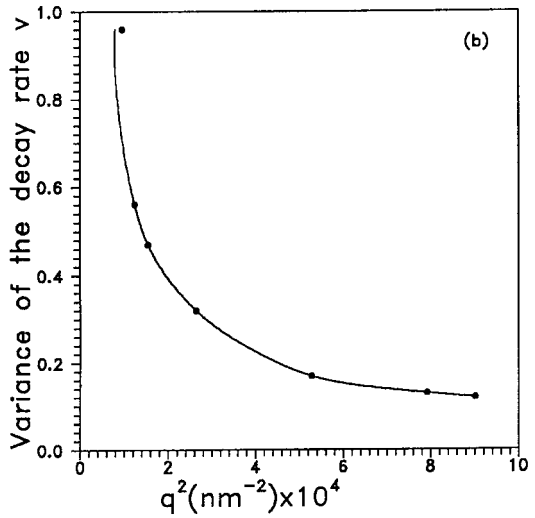

Fig. 2. Quasi-elastic measurements, presented in this figure, and intensity light scattering measurements, reported in Figure 1, have been obtained on the same sample. (a) q-dependence of the apparent diffusion coefficient deduced from cumulant analysis (dots). The triangles represent the diffusion coefficient of the smaller scatterers $D_{\rm s} = \Gamma_{\rm s}/q^2$ (see expression (12) and text). (b) q-dependence of the variance of the decay rate deduced from cumulant analysis.

The coefficients determined from this fit are $B_{\rm l} = 4.86 \times 10^{-7}$, $x = 3.16$, $B_{\rm s} = 1.06$, and $R_{\rm sgz} = 26$ nm. Moreover this treatment provides information on the fractions $A_{\rm s}(q)$ and $A_{\rm l}(q)$ of the intensity scattered by the smaller and larger scatterers

$$A_{\rm s}(q) = M_{\rm w}^{\rm app}(q_{90^\circ}) B_{\rm s}(1 - q^2R_{\rm sgz}^2/3)/M_{\rm w}^{\rm app}(q); \quad A_{\rm l}(q) = 1 - A_{\rm s}(q). \tag{9}$$

Figure 3 shows a plot of $A_{\rm s}(q)$ and $A_{\rm l}(q)$ *versus* q^2. For $q^2 \geq q_{90^\circ}^2$, the intensity scattered by the larger scatterers appears to be less than 6% of the total intensity. Quasi-elastic light-scattering measurements are compatible with the analysis done by intensity light-scattering measurements. Typical correlation functions $g(t)$ obtained at small

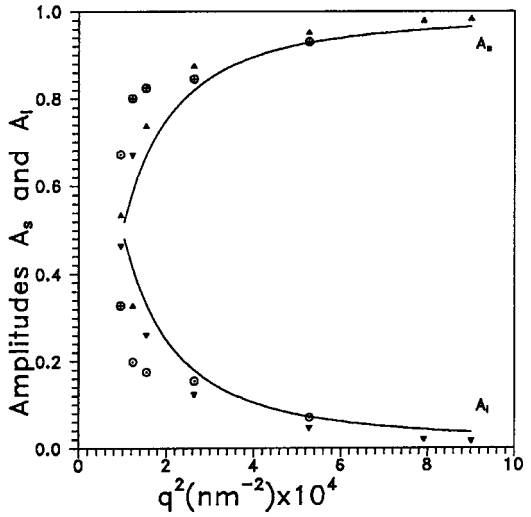

Fig. 3. q-dependence of the fractions A_s and A_l of the intensity of the light scattered by the smaller and larger scatterers, respectively. The full lines are A_s and A_l values deduced from intensity measurements (see Fig. 1). The symbols represent A_s and A_l values deduced from quasi-elastic measurements with different procedures. The full triangles and the open circles are values obtained by cumulant analysis with a floating base line (see expression (12) and text) and by the maximum entropy method, respectively.

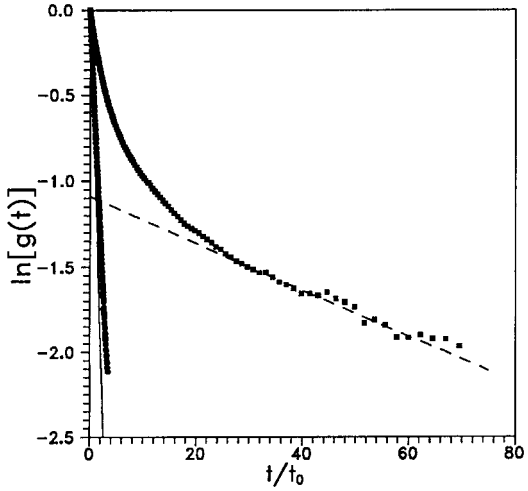

Fig. 4. Typical autocorrelation functions $g(t)$ where the squares and the dots correspond to measurements done at a scattering angle of 35° ($q = 9.8 \times 10^{-3}$ nm^{-1}) and 135° ($q = 3 \times 10^{-2}$ nm^{-1}), respectively ($c = 2 \times 10^{-2}$ wt% and salinity $= 2 \times 10^{-2}$ M) . For convenience, a reduced time scale t/t_0 where $t_0 = -(\mathrm{d}g(t)/\mathrm{d}t)_{t\to 0}$ is used in abscissa. In this representation, when functions $g(t)$ are pure exponential they should lie on the same straight line with an intercept equal to zero (full line). At 35° scattering angle, the strong curvature clearly shows a non-exponential behavior.

and large q-values are displayed in Figure 4. At small q-values, $g(t)$ clearly exhibits a non-exponential decay. Assuming a distribution of scatterers in two polydisperse populations, the correlation function $g(t)$ can be written as

$$g(t) = A_l g_l(t) + A_s g_s(t). \tag{10}$$

where $g_l(t)$ and $g_s(t)$ are the autocorrelation functions of the electric field scattered by the large and small scatterers respectively.

From the cumulant analysis in the high q range (see Figs. 2 and 3), we conclude that:

$$g(t) \approx g_s(t) = A_s[1 + v(\Gamma_s t)^2/2] \exp(-\Gamma_s t) \quad \text{with } v = 0.12. \tag{11}$$

Whatever the exact profile of $g_l(t)$ is, as t goes to zero $g_l(t) \approx 1$, and $g(t)$ can be approximated by

$$g(t) \approx A_l + A_s[1 + v(\Gamma_s t)^2/2] \exp(-\Gamma_s t) \quad \text{with } v = 0.12. \tag{12}$$

In the total q-range that we investigated, the quantities A_l, A_s and Γ_s obtained from curve fitting for different decreasing sample time spacings were extrapolated to zero time. The values of A_l and A_s deduced using this procedure are reported in Figure 3 and are in agreement with the values deduced from intensity measurements. Maximum entropy method analysis of the results confirms that the distribution, $A(\Gamma)$, of the decay rates Γ is bimodal (see Figs. 3 and 5). The results of intensity and quasi-elastic

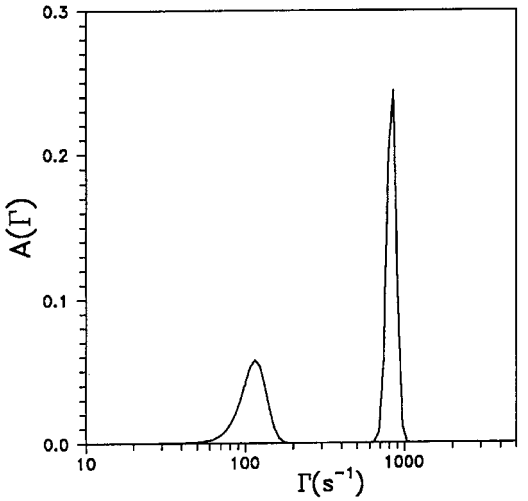

Fig. 5. Distribution of decay rates deduced by the maximum entropy method analysis from a quasi-elastic light experiment performed at a scattering vector $q = 1.1 \times 10^{-2}$ nm^{-1} (sample $c = 2 \times 10^{-2}$ wt% and salinity 2×10^{-2} M).

light scattering give consistent evidence for the presence of two types of copolymer assemblies in the solution. Let us first consider the smaller copolymer assemblies.

3.1.1 Smaller copolymer assemblies or micelles

A careful analysis of the results of the apparent diffusion coefficient of the smaller scatterers (see Fig. 2a) shows that there is a small q^2-dependence: $D_s^{app}(q) = D_{sz}(1+\varepsilon q^2 R_{sgz}^2)$

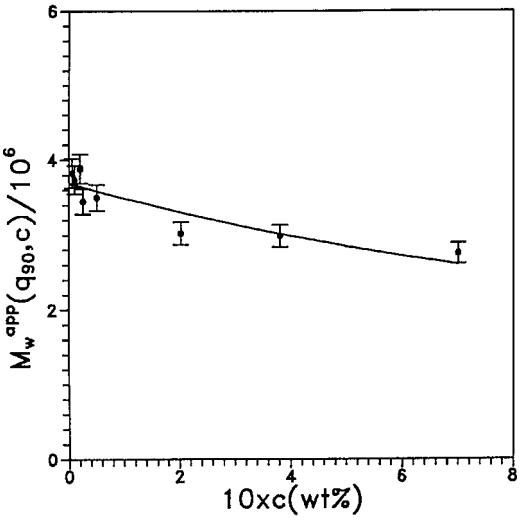

Fig. 6. Concentration dependence of the apparent weight-average molecular weight measured at scattering angle of 90°. Within experimental precision, it appears that for a salinity of 2×10^{-2} M the interactions are negligible when $c < 4 \times 10^{-2}$ wt%.

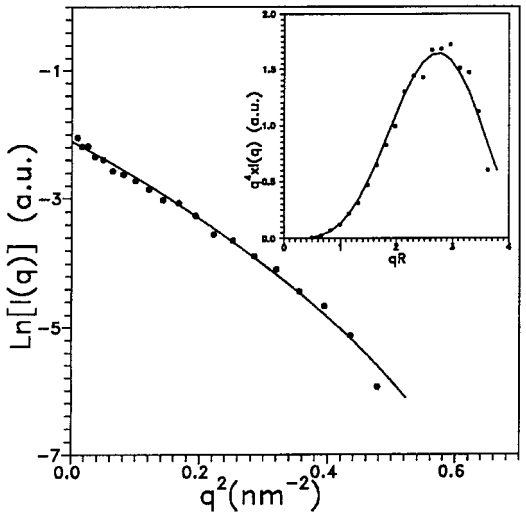

Fig. 7. Form factor of the core of micelles in H_2O/D_2O mixture $c = 1$ wt%. Experimental neutron scattering data $I(q)$ and sphere form factor (solid line) of radius $R = 5.2$ nm are presented in a Guinier representation. The inset shows the same results in Porod representation.

with $D_{sz} = 5.77 \times 10^{-12}$ m^2/s and $\varepsilon = 0.23$. The origin of the q^2-dependence is either or both the size polydispersity of micelles and the sensitivity to the dynamics of the internal modes of the micelles. The ε values deduced for different structures (stars and branched polymers) such as in [25] are between 0.1 and 0.2 which is close to the experimental value. From extrapolation to $q = 0$, using the Einstein relation we obtain $R_{shz} = 42$ nm. Experimentally, it is difficult to perfectly extract the contribution of the smaller scatterers, and we suggest that the apparent q^2-dependence can be also a residual influence of the larger scatterers. In these conditions, we believe that the best way to determine R_{shz} is to consider only the results at large q-values. From the intercept of a plot of $D_s^{app}(q)$ *versus* $1/q^2$, we obtain $D_s = 6.85 \times 10^{-12}$ m^2/s which corresponds to a size $R_{shz} = 36$ nm. We thus conclude that the smaller scatterers have a hydrodynamic size which lies between 36 and 42 nm. The hydrodynamic radius is larger than the radius of gyration $R_{sgz}(= 26$ nm) which confirms centrosymmetric structures. One has $0.6 \leq R_{sgz}/R_{shz} \leq 0.72$ a value which is close to the value 0.77 expected for monodisperse spherical particles, a result which has been also found with other similar copolymers [8]. Thus, we expect that the diblock copolymers form micelles of collapsed PEP cores with NaPSS arms. This is in full agreement with the neutron scattering results described below which enable us to determine the radius of gyration of the PEP cores.

Since the concentration of the larger copolymer assemblies w_l is very small ($w_s \approx 1$), (see Eqs. (8, 9)) an estimation of the molecular weight of the micelles can be given. Extrapolation of the light scattering measurement to infinite dilution yields $M_w^{app}(q_{90°}) = 3.7 \times 10^6$ g/mole (see Fig. 6), and thus leads to $M_{sw} = 3.9 \times 10^6$ g/mole. From this plot one can also deduce a second virial coefficient (repulsive) between micelles of order 10^5 nm^3.

The mass determination leads to an aggregation number $p = 85$. Assuming that the hydrophobic PEP core is collapsed as a melt and using the melt density value of 0.854 g/cm^3 [26], we deduce a core radius of 5.1 nm. Neutron scattering at small angles was used to directly confirm the hydrophobic association by use of the contrast matching technique. We made use of a mixture of H_2O and D_2O (44% in volume of D_2O) which matches the PSS part, making it invisible to neutrons. Results were obtained for different concentrations in polymer (0.2, 0.5 and 0.8 wt%). It was checked that in this concentration range, interactions were still negligible as confirmed by a nice superposition of the $I(q)/c$ curves (see Sect. 3.2). A typical scattering curve is shown in Figure 7, confirming directly that the scattering is fully compatible with a form factor of spheres of radius 5.2 ± 0.2 nm (aggregation number of 90). Identical results were obtained for salinities between 0 and 0.5 M within the experimental errors. An additional confirmation was obtained by means of osmotic pressure measurements (Knauer apparatus) where an estimation of p was obtained ($p \sim 60$).

3.1.2 Larger copolymer assemblies

Light scattering intensity results show that large aggregates having a size R_{lgz} larger than 100 nm exist. The exponent value 3.2 of the form factor $P_{lz}(q) \propto 1/q^{3.2}$ (see Fig. 1) permits to expect that these aggregates have a three-dimensional structure with a fractal surface.

Different profiles were tried to fit the long time tail of the correlations function $g(t)$. At the lowest q values, it is clearly established that, at long times, $g(t)$ is well described by a stretched exponential $g_l(t) \sim \exp(-(\Gamma_l t)^\beta)$

with an exponent β close to 2/3. This behavior indicates that we may probe the internal dynamics of flexible aggregates. As the intensity scattered by these aggregates strongly decreases as q increases, it was not possible to precisely establish the q-dependence of Γ_1. However when internal dynamics is probed, a relationship exists between the exponent value β and the q-dependence of the decay rate [27]: $\Gamma_1 \sim q^{2/\beta}$. At the sight of the β value, it is reasonable to assume that $\Gamma_1 = A' k_B T q^3/6\pi\eta$ where A' is a numerical factor. At $q = 9.77 \times 10^{-3}$ nm^{-1}, we find $\Gamma_1 \sim 38$ s^{-1} which leads to a value $A' \sim 0.15$. This A' value is low in comparison to the values found for neutral polymers. Whatever the architecture of the polymer (starlike, branched or linear), A' is of the order of unity [27]. Another possibility is that the apparent stretched exponential profile of the long time tail reflects only a strong polydispersity in size of non flexible aggregates. Applying the Einstein relation $\Gamma_1 = k_B T q^2/6\pi\eta R_{\rm lhz}$, one deduces that the mean hydrodynamic radius $R_{\rm lhz}$ of the larger scatterers is of the order of 620 nm.

The nature of the large aggregates is still conjectural, one possibility being the existence of supra-micellar structures which are starlike micelles held together by residual non- sulfonated segments of their corona chains. Note that the chain extremities are indeed non- sulfonated ones (secbutyl groups) and consequently are highly hydrophobic. This could favor some kind of association between micelles through the extremities of the corona. However, we believe that these aggregates are not due to residual low-molecular impurities since we recovered the same quantitative results depicted above after dialysis of the polymer.

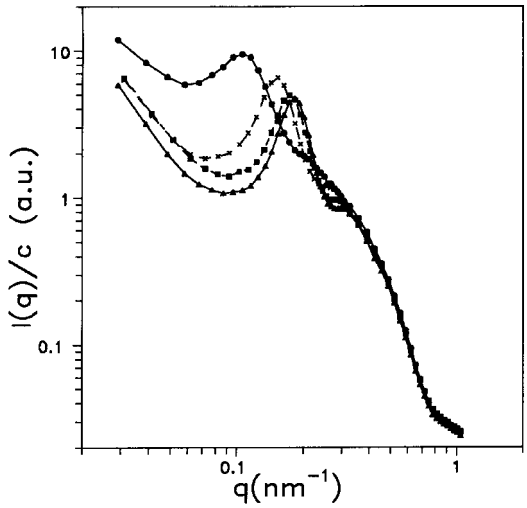

Fig. 8. Neutron scattered intensity $I(q)/c$ from samples, in D_2O solvent without added salt, at different concentrations: 5 wt% (dots); 10 wt% (crosses); 15 wt% (squares); 20 wt% (triangles).

3.2 Concentrated solutions

Some preliminary light-scattering experiments were performed in the concentration range $1 < c < 10$ wt% on solutions without salt. It appears that the results cannot be analyzed assuming a single photon process. The large increase of the depolarization factor with the concentration indicates the apparition of multiple scattering. The depolarization factor (ratio of the light intensity polarized horizontally to the vertically polarized intensity) was found to be 3.3×10^{-3}, 7.2×10^{-3}, and 3.5×10^{-2} for samples of concentrations 10^{-2}, 1, and 10 wt%, respectively. Thus we have been lead to investigate the concentrated regime using X-ray and neutron scattering techniques which are more appropriate.

A range of concentration in polymer from 0.2 to 20 wt% (D_2O solvent) without added salt has been studied. It can be seen in Figure 8 that a correlation peak is obtained within a range of concentration 5-20 wt% in a representation $I(q)$ *versus* q, where $I(q)$ is the neutron scattered intensity and q the wavevector. We then interpret this correlation peak as the signature of liquid-like correlations between micelles. The first sharp occurrence of this peak at a concentration about 5 wt% is related to the crossing of the concentration c^* where the arms of the micelles begin to contact. This concentration is roughly estimated knowing the aggregation number ($\sim$ 85) thanks to light and neutron scattering measurements and the hydrodynamic radius of an isolated micelle as determined by QELS ($\sim$ 38 nm) which gives $c^* \sim 2$ wt% by using the maximum packing fraction for randomly organized spheres in three dimensions (~ 0.64). The value of q^* for c^* can be extrapolated from the results at higher concentrations, giving $q^* = 8.2 \times 10^{-2}$ nm^{-1} and leading to $1/2(2\pi/q^*) = 38$ nm in agreement with the radius of the micelles. For higher concentrations the increase in q^* denotes either a contraction of the arms or an interpenetration of them. Comparison of the scattering curves at various concentrations also shows that the scattering intensities are nicely superimposable when expressed in the I/c *versus* q representation in the q range ($3.2 \times 10^{-1} - 1.0$ nm^{-1}), a feature which means that spatial scales less than 3.1 nm are essentially unperturbed by interactions. This is probably due to the unchanged geometry of the core (radius about 6 nm) and of the inner segments of the corona even if interpenetration or contraction occurs.

It is worth comparing these results with the evolution of the so-called polyelectrolyte peak which is observed by neutron or X-ray scattering on solutions of NaPSS [15]. This peak — for sufficiently high concentrations — evolves as $q^* \propto c^{1/2}$ for highly sulfonated NaPSS [15] and has an absolute value which, for the same concentration of NaPSS and diblock and nearly the same molecular weight (a parameter which does not shift the peak much for polyelectrolyte), lies an order of magnitude above the one we observed. Moreover it can be observed that for concentrations above 10 wt%, the polyelectrolyte peak nearly vanishes while the diblock peak is still well defined. It must be noted that although the polyelectrolyte peak is preserved upon dilution and thus observable by light scattering [28], we never observed such a peak for dilute solutions of diblocks. We thus interpret our results as the signature of a micellar packing. This is confirmed by plotting

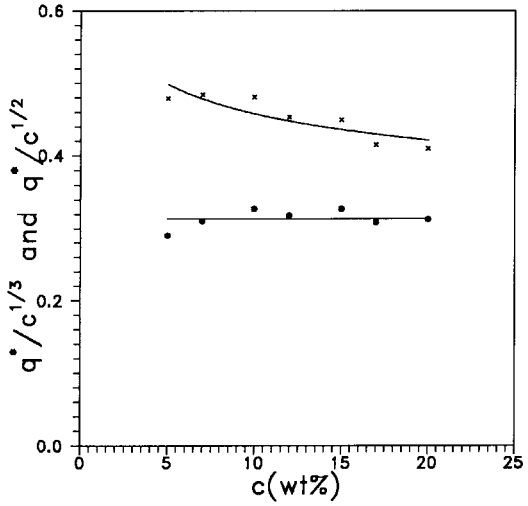

Fig. 9. Variation of the peak position q^* (samples without salt): $c^{1/3}$ dependence (dots) and $c^{1/2}$ dependence (crosses) as a function of the concentration. The wavector q^* cannot be described by a $c^{1/2}$-dependence.

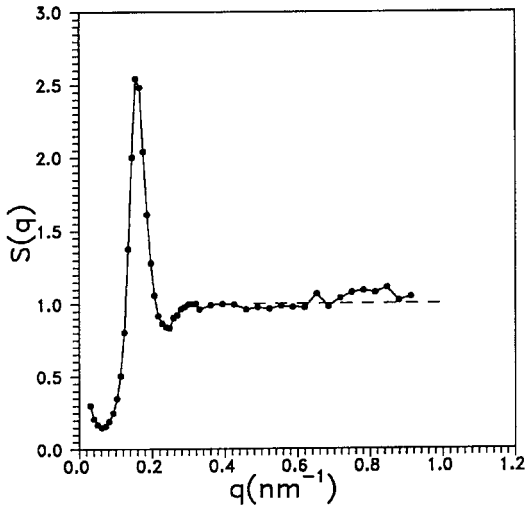

Fig. 10. Typical structure factor $S(q)$ deduced from neutron scattering measurements (c = 10 wt%, D_2O solvent without added salt).

the variation of the peak position q^* (maximum of $I(q)$) with c in the range 2 to 20 wt% (Fig. 9) which is well fitted by the law $q^* \propto c^a$ with $a = 0.36 \pm 0.04$. The value of the exponent a is compatible with 1/3, the value expected for the evolution of a liquid order with concentration [16,29].

If we assume that a form factor of the micelles, $P(q)$, can be defined in the studied q-range the scattered intensity can be written as $I(q) \propto cP(q)S(q)$ where $S(q)$ is a structure factor which can be obtained by $I/[cI(c = 1\%)]$ where c is expressed in wt%. This expression assumes that $I(c = 1\%)$ represents correctly the form factor (dilute concentration). We checked that point by inspecting different dilute concentrations (0.2, 0.5 and 1 wt%) where a single shape of $I(q)/c = P(q)$ was recovered. Such typical $S(q)$ are shown in Figure 10 and have the nice trend to go to 1 for large q which, in some sense, validates the hypothesis of the existence and definition of $P(q)$, at least in the high q range. This allows inspection of the variation of the peak position q^* (now defined as the first maximum of $S(q)$) over the concentration range 5 to 20 wt% which is well fitted by the law $q^* \propto c^a$ with $a = 0.33 \pm 0.02$, again indicating a liquid order of micellar objects.

The amplitude $S(q^*)$ is found constant (within the experimental uncertainties) in the range of concentration 7-20 wt%. We do not observe any decrease of $S(q^*)$ with c contrary to what has been reported for neutral stars [29] when interpenetration of arms occurs. In this latter case, contact of the arms generates a discontinuity in the osmotic pressure which induces the maximum of $S(q^*)$ and one expects more destructive interferences between both segments and cores to occur as long as interpenetration occurs, leading to a disappearance of the correlation peak with concentration. Our results are then inconsistent with the hypothesis of interpenetrated arms.

Another hypothesis is the contraction of the micelles above c^*, the micelles staying densely packed in the whole concentration range above c^*. In this case, we ignore the evolution of the form of the micelles with concentration and we can only discuss the total scattered intensity. However the correct behavior of the $S(q)$ deduced by the above procedure is not contradictory since such a contraction is likely to modify the form factor of a micelle only at low q values. As a matter of fact one can imagine that a contraction of the arms means that the structure evolves from a perfect rod towards a rod having a finite persistence length, making the chain more contracted at large spatial scales. Thus, it is not surprising to preserve a meaningful behavior of the $S(q)$ at large q values where the segment statistics stays rod-like [30]. The hypothesis of non-penetrable packed micelles enables an independent determination of the micellar aggregation number to be given for the range where the correlation peak is determined. This determination is based on the assumption that the micelles are packed like randomly organized spheres showing liquid-like order. Then, the volume fraction ϕ_c occupied by the micelles is the maximum packing fraction for randomly organized spheres in three dimensions ($\phi_p \sim 0.64$) and also writes $(\rho c/M)(4/3\pi R^3)$ where ρ is the solvent density (D_2O), c is the concentration in wt% and M is the mass of the micelle. Thus, M can be determined from each couple (c, q^*), since $R = \pi/q^*$, and we obtain an average value of $p = 90$ in perfect agreement with our previous determinations.

Addition of monovalent salt (NaCl) has little effect on the existence and position of the peak in $I(q)$. It is shown in Figure 11 that for a concentration of polymer of 15 wt%, the peak obtained from neutron scattering is slightly shifted to lower values as the salt concentration (or ionic strength) reaches 0.5 M. A rough calculation can be made about the inner counterion concentration within a micelle, assuming that all the counterions are localized inside the micelle. For a radius R_0 of 39 nm which corresponds to isolated micelles one gets an inner counterion concentration of 0.05 M. For a concentration of 15 wt%,

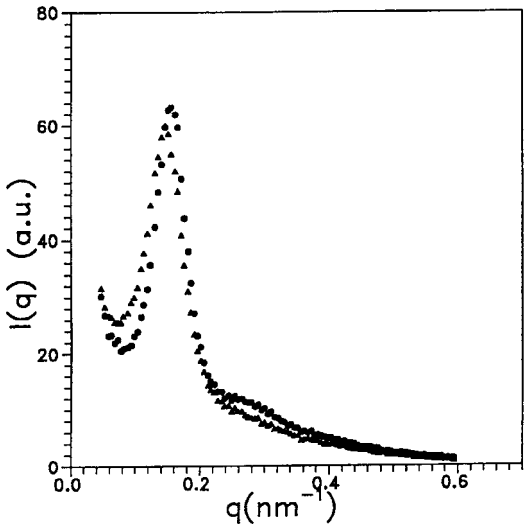

Fig. 11. Typical variation of neutron scattering intensity $I(q)$ when salt is added ($c = 15$ wt%, D_2O solvent). Salt concentrations: 0.01 M (dots); 0.5 M (triangles).

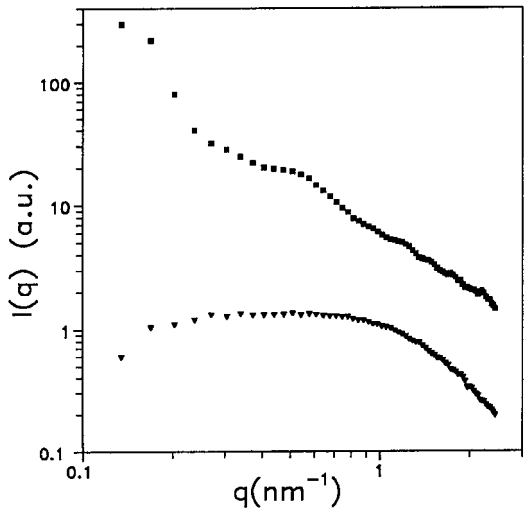

Fig. 12. X-ray scattering intensity $I(q)$ from samples in H_2O solvent at a concentration of 10 wt% and a salinity 0.1 M. The squares and the triangles represent the results obtained with the copolymer (PEP/PSSNa; $M_W = 4.7 \times 10^4$) and an homopolymer (PSSNa; $M_W = 4.6 \times 10^4$), respectively.

assuming that the micelles are then contracted by a factor of 2 given by the value of q^* at this polymer concentration ($2\pi/q^* \approx R_0$ neglecting the dimension of the PEP core), one obtains a counterion concentration of 0.4 M (ionic strength of 0.2 M). It is then understandable that the effect of added salt only occurs for added concentrations of order 0.5 M. This is reminiscent of similar behaviors obtained for solutions of charged silica or latex particles where the ordering peak is nearly unchanged in position by addition of salt [16]. In these latter cases, however, the height of the peak strongly decreases upon addition of salt. On the contrary, in our case, the height of the ordering peak only slightly decreases when the added salt concentration reaches an ionic strength comparable to the one inside the micelles. For each polymer concentration, the scattered intensity at low q values increases when some threshold in electrolyte is exceeded. The additional screening of the micellar interactions by the electrolyte overcomes the already large screening due to the counterions brought by the diblock itself. More specifically, we also investigated the differences between the scattered signal due to the diblock and the signal scattered by X-rays for a salted solution of homopolyelectrolyte PSSNa. It is clear from Figure 12 that for identical concentrations of diblock and PSSNa (10 wt% in 0.1 M of salt) of comparable molecular weight, an ordering peak of PSSNa is no longer observed while the ordering peak of the diblock still persists.

4 Summary and conclusion

This paper shows, in a first part, that the recurrent problem of large aggregates coexisting with a micellar population of water soluble polymers can be quantitatively addressed. An important consequence is that, despite the presence of these aggregates, the existence and characteristics of the micellar population can be assessed by a careful procedure based on light scattering. It must be noted that the existence of such micelles is now evidenced by different techniques. The study of more concentrated solutions leads to the occurrence of ordering between micelles. This order is very similar to the packing of spheres, exhibiting a liquid-like order on a wide range of concentrations. However it is not clear at the moment whether a crystalline phase of such micelles can exist or not in some range of the concentration and ionic strength. The generalization to other polymer architecture (molecular weight, chemical nature of the monomers) particularly deserves interest. The mechanism of contraction of the arms is also worthy of further study, especially if the chain conformation during this contraction can be followed. Such an attempt is currently in progress.

We thank P. Lixon and S. Désert for numerous discussions, measurements of refractive index increments and characterization of potential impurities. J. Teixeira is also warmly thanked for the use of the PAXE spectrometer, M. Olvera de la Cruz for many discussions and J. Langowski for kindly providing us the MEXDLS program (maximum entropy program) he designed. P.G., J.W.M. and M.T. acknowledge the support of the NATO CRG ♯930892. J.W.M. and M.T. also thank the National Science Foundation, CTS and DMR Programs, for support (Grant NSF/CTS-9107025).

References

1. A. Halperin, M. Tirrell, T.P. Lodge, Adv. Polym. Sci. **100**, 31 (1991).
2. C. Amiel, M. Sikka, J.W. Schneider, Y.H. Tsao, M. Tirrell, J.W. Mays, Macromol. **28**, 3125 (1995).

3. P. Guenoun, A. Schalchli, D. Sentenac, J.W. Mays, J.J. Benattar, Phys. Rev. Lett. **74**, 3628 (1995).
4. A recent review is: M. Moffitt, K. Khougaz, A. Eisenberg, Accounts of Chemical Research **29**, 95 (1996).
5. J. Selb, Y. Gallot, *Developments in Block Copolymers*, edited by I. Goodman (Elsevier, London, 1985) pp. 27-96.
6. D. Kiserow, K. Prochazka, C. Ramireddy, Z. Tuzar, P. Munk, S.E. Webber, Macromol. **25**, 461 (1992).
7. K. Khougaz, I. Astafieva, A. Eisenberg, Macromol. **28**, 7135 (1995).
8. P. Guenoun, H.T. Davis, M. Tirrell, J.W. Mays, Macromol. **29**, 3965 (1996).
9. X.F. Yuan, A.J. Masters, C. Price, Macromol. **26**, 6876 (1992).
10. C. Huang, M. Olvera de la Cruz, M. Delsanti, P. Guenoun, accepted to Macromol.; N. Shusharina, M.V. Saphonov, I.A. Nyrkova, P.G. Khalatur, A.R. Khokhlov, Ber. Bunsenges. Phys. Chem. **100**, 857 (1996).
11. A. Qin, M. Tian, C. Ramireddy, S.E. Webber, P. Munk, Z. Tuzar, Macromol. **27**, 120 (1994).
12. see reference 11 for charged systems and for neutral ones see: R. Xu, M.A. Winnik, F.R. Hallett, G. Riess, M.D. Croucher, Macromol. **24**, 87 (1991).
13. E.B. Zhulina, O.V. Borisov, Macromol. **29**, 2618 (1996); O.V. Borisov, J. Phys. II France **6**, 1 (1996).
14. P. Pincus, Macromol. **24**, 2912 (1991).
15. M. Nierlich, C. Williams, F. Boué, J.P. Cotton, M. Daoud, B. Farnoux, G. Jannink, C. Picot, M. Moan, C. Wolff, M. Rinaudo, P.G. de Gennes, J. Phys. France **40**, 701 (1979).
16. P.N. Pusey, in: *Les Houches: Liquids, Freezing and Glass Transition*, part II (North-Holland, 1991); M. Delsanti, J. Chang, P. Lesieur, B. Cabane, J. Chem Phys. **16**, 7200 (1996); J. Chang, P. Lesieur, M. Delsanti, L. Belloni, C. Bonnet-Gonnet, B. Cabane, J. Phys. Chem. **99**, 15993 (1995); W. Härtl, H. Versmold, U. Wittig, V. Marohn, Molecular Physics **50**, 815 (1983); J.W. Goodwin, R.H. Ottewill, J. Chem. Soc. Faraday Trans. **87**, 357 (1991)
17. J. Podesva, P. Spacek, C. Konak, J. Appl. Polym. Sci. **44**, 527 (1992); P.L. Valint, J. Bock, Macromol. **21**, 175 (1988).
18. J. Mays, N. Hadjichristidis, L.J. Fetters, Macromol. **17**, 2723 (1984).
19. see for instance B. Chu, *Laser Light Scattering* (Academic Press, Inc. New York, second edition, 1991).
20. J. Langowski, R. Bryan, Macromol. **24**, 6346 (1991).
21. E. Moreels, W. De Ceuninck, R. Finsy, J. Chem. Phys. **86**, 618 (1986); *Instruction Manual of the Brookhaven goniometer* (1991).
22. F. Né, D. Gazeau, J. Lambard, P. Lesieur, Th. Zemb, A. Gabriel, J. Appl. Cryst. **26**, 763 (1993).
23. $\mathrm{d}\Sigma_\mathrm{w}/\mathrm{d}\Omega = (1 - T_\mathrm{w})/f4\pi t_\mathrm{w}$ where the factor f takes into account the fact that the incoherent scattering of the water is not rigorously isotropic. The factor f depends on wavelength λ and for numerical f values see for instance: G.D. Wignall, F.S. Bates, J. Appl. Cryst. **20**, 28 (1987); B. Jacrot, Rep. Prog. Phys. **39**, 911 (1976).
24. *Light Scattering from Polymer Solutions*, edited by M.B. Huglin (Academic Press London, 1972).
25. W. Burchard, M. Schmidt, W.H. Stockmayer, Macromol. **13**, 1980 (1265).
26. J. Gottro, Ph. D. thesis, Northwestern University (1982).
27. M. Adam, M. Delsanti, J. Phys. Lett. France **38**, l (1977); A. Lapp, T. Csiba, B. Farago, M. Daoud, J. Phys. II France **2**, 1495 (1992); M. Delsanti, J.P. Munch, J. Phys. II France **4**, 265 (1994); G.S. Grest, L.J. Fetters, J.S. Huang, D. Richter, Advances in Chemical Physics, **XCIV**, edited by I. Prigogine, S.A. Rice (John Wiley & Sons, Inc. 1996).
28. M. Drifford, J.P. Dalbiez, J.Phys. Chem., **88**, 5368 (1984).
29. T.A. Witten, P.A. Pincus, M.E. Cates, Europhy. Lett. **2**, 137 (1986); D. Richter, L. Jucknischke, L. Willner, L.J. Fetters, M. Lin, J.S. Huang, J. Roovers, C. Toporovski, L.L. Zhou, J. Phys. IV France **3**, 3 (1993).
30. P. Guenoun, F. Muller, M. Delsanti, L. Auvray, Y.J. Chen, J.W. Mays, M. Tirrell (to be published).